Title

Nucleophilic substitution between polysulfides and binders unexpectedly stabilizing lithium sulfur battery

Authors

Ling, Min
Zhang, Liang
Zheng, Tianyue
et al.

Publication Date

2017-08-01

DOI

10.1016/j.nanoen.2017.05.020

Peer reviewed

Nucleophilic Substitution Between Polysulfides and Binders Unexpectedly Stabilizing Lithium Sulfur Battery

Min Ling[1], Liang Zhang[2], Tianyue Zheng[1], Jun Feng[2], Jinghua Guo[2], Liqiang Mai[3], Gao Liu[1]*

[1]Applied Energy Materials Group, Energy Storage and Distributed Resources Division, Lawrence Berkeley National Laboratory, Berkeley, California 94720, United States of America.
[2]Advanced Light Sources, Lawrence Berkeley National Laboratory, Berkeley, California 94720, United States of America.
[3]State Key Laboratory of Advanced Technology for Materials Synthesis and Processing, Wuhan Univerisity of Technology, Wuhan 430070, China.

Keywords: Nucleophilic substitution, poly(vinyl sulfate), carrageenan, chemical binding, high loading electrodes, lithium sulfur battery.

Abstract: Polysulfide shuttling has been the primary cause of failure in lithium-sulfur (Li-S) battery cycling. Here, we demonstrate an uncleophilic substitution reaction between polysulfides and binder functional groups can unexpectedly immobilizes the polysulfides. The substitution reaction is verified by UV-visible spectra and X-ray photoelectron spectra. The immobilization of polysulfide is *in situ* monitored by synchrotron based sulfur K-edge X-ray absorption spectra. The resulting electrodes exhibite initial capacity up to 20.4 mAh/cm^2, corresponding to 1199.1 mAh/g based on a micron-sulfur mass loading of 17.0 mg/cm^2. The micron size sulfur transformed into nano layer coating on the cathode binder during cycling. Directly usage of nano-size sulfur promotes higher capacity of 33.7 mAh/cm^2, which is the highest areal capacity reported in Li-S battery. This enhance performance is due to the reduced shuttle effect by covalently binding of the polysulfide with the polymer binder.

1. Introduction

Over the past decades, a strong demand for low-cost and high-energy-density rechargeable batteries has spurred lithium-sulfur (Li-S) rechargeable battery research. Rechargeable Li-S batteries have great commercial potential for two reasons. First, sulfur is an abundant and low-cost material. Second, the Gibbs energy of the lithium (Li) and S reaction is approximately 2,600 Wh/kg, assuming the complete reaction of Li with sulfur to form Li_2S, more than five times the theoretical energy of transition metal oxide cathode materials and graphite coupling. With these advantages, Li-S batteries could be both high energy density and low cost, satisfying demand in both stationary energy storage and transportation application. [1-2] Despite its advantages, the use of rechargeable Li-S batteries is still very limited. Obstacles include the low conductivity of sulfur and the loss of sulfur cathode material as a result of polysulfide dissolution, which causes a shuttle effect and significant capacity fading. [3-4] Theoretically, the octasulfur (cyclo-S_8) is reduced by steps to solid Li_2S during lithiation in the sulfur cathode. During this process, electrolyte soluble Li_2S_x are generated when the x value ranges from 8 to 4. The soluble lithium polysulfides diffuse through the electrolyte and further reduced at the lithium metal side to form low-order of polysulfide. The partially reduced and soluble polysulfides can diffuse back to the sulfur electrode side, which are oxidized to higher-order of polysulfides at the cathode side during the delithiation process.[5] This shuttle effect, together with low conductivity, leads to poor sulfur utilization and fast-capacity fade, which have hindered widespread use of rechargeable Li-S batteries. [6-7]

Efforts to trap the shuttling polysulfides have mainly focused on meso/nano-carbon matrix as summarized by Liu et al., [8-20] formation of sulfur composites initiated by Wang et al. [21-23] and metal oxide/sulfide hosts reviewed by Mai et al.[24] Since divinyloxyhydroxyolysulphides was first developed by T.A. Skotheim et al. as an alternative binder solution for Li-S batteries,[25] polymers including gelatin,[26-28] polyethylene oxide,[29] polyacrylic acid,[30] carboxyl methyl cellulose,[31] polyvinylpyrrolidone[32], gum arabic binder, [33] carbonyl-β-cyclodextrin[23] and polyamidoamine dendrimer[34] were identified as promising binders to address the issue. Besides the better dispersion and distribution properties of the emerging binders, as revealed by Cui et al.,[32] the existence of carbonyl groups in the emerging binders play a pivotal role in

the improved cycle performance. The electron-rich oxygen with lone pairs is favourable to form lithium-oxygen (Li-O) bond with lithium polysulfides. The contribution of carbonyl groups and surface modification effect was also evidenced by our group through poly (9, 9-dioctylfluorene-co-fluorenone-co-methylbenzoic ester) (PFM) binder. [35]

An alternative method to provide strong binding with polysulfide is through a covalent bond between the electrode and sulfur species. A nucleophilic substitution reaction between the dissolved polysulfides and leaving groups on the polymer binder can fix the polysufides on to the electrode via the newly formed C-S covalent bond. A number of factors govern reactivity in a nucleophilic reaction: the ability of both the nucleophile and the leaving group to polarize, the stability of the leaving group, and the interaction between the nucleophile and leaving group [36]. To capture the polysulfide in a timely manner, the choice of leaving group is critical. A good leaving group must be able to stabilize a large negative charge in both the transition state and the product stage. A good measure of anion stability is the pK_a of an anion's conjugate acid, with the lower pK_a being associated with a better leaving group [36]. Considering the unique requirements of the Li-S batteries, the leaving group also must not introduce reactive species into the system. Based on these requirements, the sulfate leaving group is adopted. (Fig. 1A).[34] Synthetic poly(vinyl sulfate) potassium salt (PVS), a commonly used synthetic polymer, has a sulfate rich chemical structure that can be well controlled and would be an ideal polymer to form a composite. However, the binding strength of PVS is inadequate when used as a binder to form a composite electrode. In contrast, carrageenan, a material derived from polysaccharides in seaweed [37], has desirable features for binders such as aqueous solubility, high adhesiveness, variable concentrations of sulfate leaving groups, biodegradability, and nontoxicity. The density of sulfate groups on carrageenan controls the gelation process [38] and the extended hydroxyl groups are indigent to the polysaccharide structure, providing an extended interaction with the surrounding polar aqueous environments. Nature has inadvertently designed carrageenan to be an ideal material for sulfur electrode binder applications. It not only possesses the sulfate leaving groups to capture sulfides, but also has rich hydroxyl groups for adhesion to form stable conductive networks with carbon black conductive additives and interaction with polar electrolyte. Carrageenan has much greater adhesion and sulfate functionality as a leaving group. Carrageenan should

have an even better chemical reactivity with polysulfide than PVS, due to some of the sulfate groups on the primary carbon sites.

2 Results and discussion

2.1 Nucleophilic substitution reaction in the electrode.

In this research, initial efforts are focused on PVS with a sulfate leaving group and polyethylene type backbone[39]. Ultraviolet-visible spectroscopy (UV-vis) is conducted to confirm the polysulfide immobilization capability of the polymers as shown in Fig. 1. The 0.1 g polymer is soaked in the 1-mL 3-mmol/L long-chain lithium polysulfide (average formula Li_2S_6) in 1,3-dioxolane (DOL)/ 1,2-dimethoxyethane (DME) solution for 24 hours to track the polysulfide substitution evolution. This design allows polysulfide to continuously be captured by the electrode via a chemical substitution reaction. Li polysulfide is a strong nucleophile [40], which can attack active carbon (C) sites attached to good leaving groups. This nucleophilic substitution reaction results in the formation of a new C-S bond with the departure of the leaving group. PVS is a liner polymer with sulfate functional groups, which is a very good leaving group during a nucleophilic substitution reaction with polysulfide [41-42] (Fig. 1A). The *in situ* spectra indicate that Li_2S_6 species produce characteristic peaks in around 430 nm (Fig.

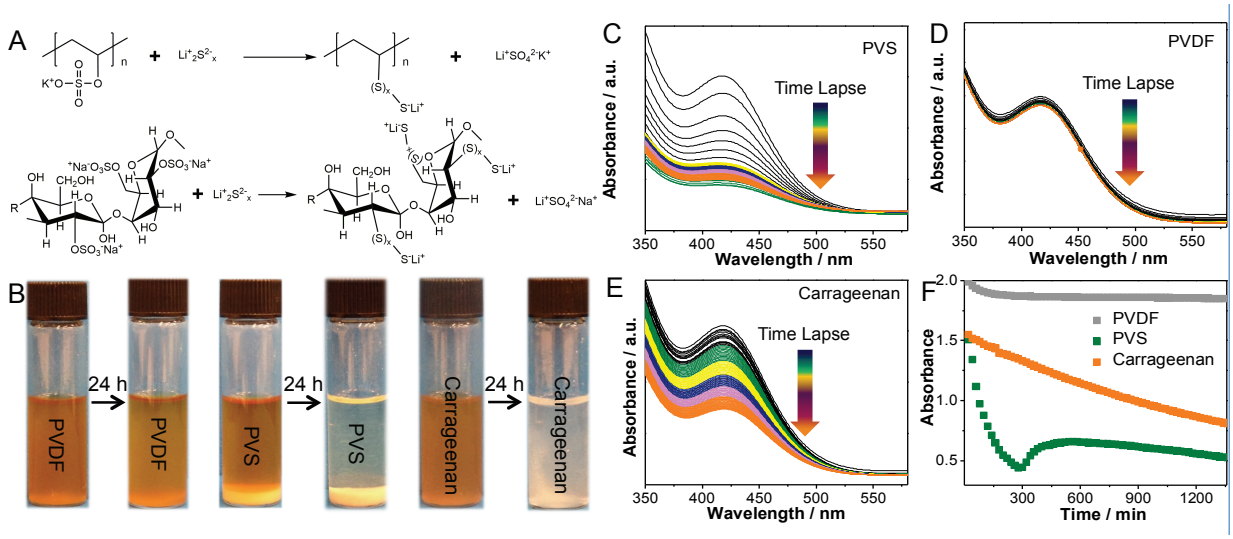

Fig. 1. The polymers with chemical leaving groups can react with polysulfide. (A) Molecular structures of PVS and natural product of carrageenan and their replacement reactions with polysulfide to form immobilized polysulfides on the polymer backbones. (B) Visual effects of the polysulfide solution exposed to different binders over 24 hrs. (C,D,E) The time-lapsed UV-*vis* absorbance of *in situ* UV-*vis* spectra of PVS, PVDF and carrageenan in 3 mmol/L Li polysulfide in DOL/DME solution. (F) UV-vis absorbance changes with time of the three polymer binders.

1 C, D, E).[43] The full spectra and reaction kinetics are demonstrated in Fig. S3. A significant polysulfide concentration decrease is recorded for the solution exposed to PVS polymer within 3 hours. In contrast, the absorption signals for polysulfide solution exposed to PVDF hold constant, indicating limited substitution of PVDF with polysulfide over 24 hours. When the PVS polymer is exposed to the electrolyte with polysulfide, the nucleophilic attack of the polysulfide to the PVS causes the instant formation of the oligosulfide crosslink PVS network structure, leading to the rapid depletion of polysulfide in the electrolyte phase. Fig. 1B and 1C show the rapid removal of polysulfide in the electrolyte, as the UV visible spectra of the electrolyte solution show rapid dwindling of the polysulfide absorption peak when exposed to the PVS polymer. In comparison, PVDF does not have good leaving group, [44-46] therefore polysulfide stays in the electrolyte as shown in Fig. 1B and D. Fig. 1B shows the visual color changes after the introduction of PVS into the polysulfide-containing electrolyte. The reaction between polysulfide and the functional PVS polymer is confirmed not only by the decrease of polysulfide concentration in the presence of PVS, but also by the formation of S-S and C-S bonds in the PVS polymer through the appearing peak located at 2472.7 and 2473.7 respectively, in the synchrotron-based sulfur K-edge X-ray absorption spectra (XAS) [47] (Fig. 2A). The spectra clearly confirm the formation of the C-S bonds and the presence of the S-S bonds in the PVS polymer when exposed to the polysulfide containing electrolyte.

However, PVS does not form a mechanically robust polymer composite laminate with carbon black and sulfur particles. The electrode made with PVS lacks mechanical strength, a major drawback for a composite electrode (Fig. 2B). From a more practical standpoint, a polymer with improved adhesion to form conductive network structures would be more desirable, in addition to a polymer that can *in situ* react with polysulfide. Carrageenan is a natural polymer with sulfate groups, and polyol functional groups, which are ideal for adhesions [38]. As a natural product, carrageenan is water-soluble; all electrode processing can be done in aqueous media. Although carrageenan has a more complex structure than that of the PVS, similar *in situ* grafting and crosslinking reactions can occur between the polysulfide and carrageenan polymer (Fig.1A, B, E, F). As expected, the absorption intensity of the polysulfide solution decreased (Fig. 1E) when the polysulfide solution is exposed to the carrageenan polymer, corresponding to the substitution reaction of sulfate groups with

dissolved polysulfide to form grafted polysulfide on the carrageenan polymers. The signature dark yellow color of polysulfide solution transforms to clear solution when the powder of carrageenan is added into the solution (Fig. 1B). The plots in Fig. 1F show rapid consumption of polysulfide using both PVS and carrageenan, but the concentration of polysulfide stays at a high level when PVDF is added to the polysulfide solution and after extended exposure times. Although PVS shows fast polysulfide capturing in Fig. 1F when polymer powders are used, the actual rate of capture in the electrode for both polymers would depend on the morphology and distribution of the polymer binder. The morphology and distribution of the polymer binder will be discussed after the cycling performance.

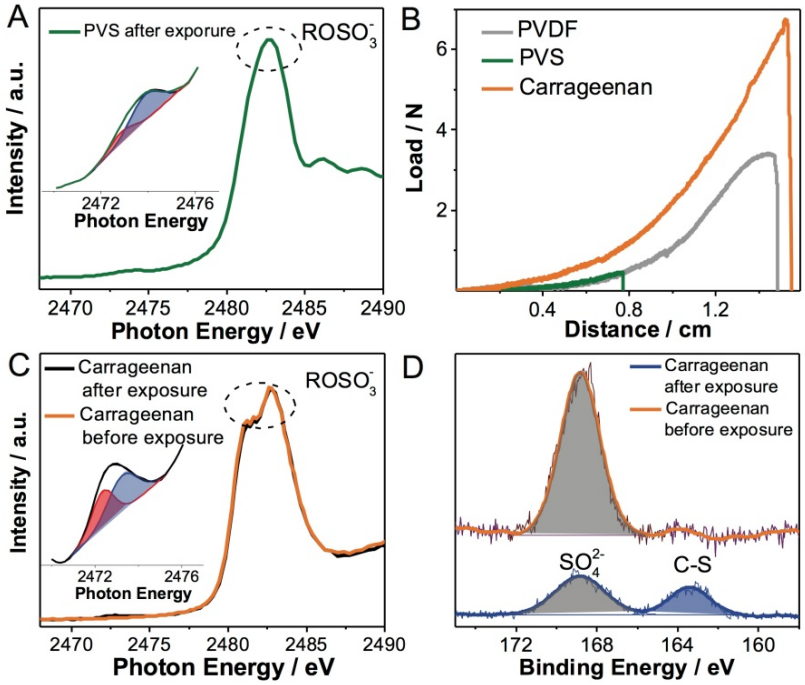

Fig. 2. Advanced spectroscopic characterization of the C-S bond formations of the polymer binders, and the binder adhesion strength. (A) Sulfur K-edge XAS spectra of the PVS film after exposure to the polysulfide solution show the formation of C-S and S-S bond. The inset curve is the enlargement of the main curve, where the bonds of C-S and S-S overlapped. The bottom blue and red shadows are mathematically fit of C-S and S-S bond, respectively. (B) Adhesion strength of the composite electrodes evaluation through peel test. (C) Sulfur K-edge XAS of carrageenan film before and after exposure to polysulfide solution. The C-S and S-S bonds appear after the exposure. (D) XPS for carrageenan film before and after exposure to polysulfide solution. In both PVS and carrageenan cases, the XAS spectra and XPS confirm the formation of C-S bonds between the polymer binders and polysulfide.

As demonstrated by UV-vis spectroscopic experiments, the reaction of polysulfide with either PVS or carrageenan results in the fixation of the polysulfide. When polysulfide reacts with polymers, it acts as a crosslink agent to form network polymers [48]. Further

reduction of grafted polysulfide leads to the breaking of the S-S bonds and the formation of insoluble short chain Li_2S_n ($n < 4$) [6]. To study the chemical bondage after immobilization, we applied synchrotron-based S K-edge absorption spectra (XAS) and X-ray photoelectron spectra (XPS) to monitor the formation of C-S chemical bonds in polymers after nucleophilic substitution as shown in Fig. 2. S-S and C-S bonds, corresponding to 2472.7 and 2473.7 eV [47-49], are observed in PVS thin film exposed to polysulfide as shown in Fig. 2A. A detailed investigation is conducted of the carrageenan polymer before and after exposure to the polysulfide solution (Fig. 2C, D). The total fluorescence yield (TFY) spectra of PVS and carrageenan all have a prominent peak at 2482.5 eV, which is attributed to the R-OSO_3^- Sσ* [33]. This XAS feature remains the same in regards to the peak position and intensity before and after exposure, which indicates the R-OSO_3^- specie exist before and after the polysulfide grafting. The emerging peak at 2472.7 and 2473.7 eV after the film exposure to the polysulfide solution confirms the existence of S-S and formation of C-S bond in the bulk material. One may notice that the peak intensity of S-S and C-S is much lower than that of R-OSO_3^-, which is an intrinsic character of the XAS. The white line intensity depends on matrix elements and occupancy of any bound final states [50-51]. The rising edge XAS visible as the features at 2472.7 (S-S) and 2473.7 eV (C-S) is the low valent sulfur, while the high valent sulfur (R-OSO_3^-) XAS maximizes near 2483.5 eV [52]. The relative weight comparison of S-S and C-S *vs*. R-OSO_3^- can be reflected more accurately in the XPS that investigate the chemical bondage for carrageenan in Fig. 2D. A new peak at 163.2 eV ascribed to the C-S bond appears after nucleophilic reaction. In the Li-S battery with sulfate rich binders, this reaction, i.e., the formation of C-S bond, is electrochemically initiated during the first few cycles when polysulfide forms. Polysulfide is captured in the S electrode to alleviate the polysulfide dissolution and shuttle effect. The advantages of this approach are two-fold. First, the sulfate rich polymers are able to immobilize the polysulfide dissolved in the electrolyte; second, since the polymer binds conductive carbon to form a conductive network, the immobilized polysulfide is within the electron tunneling distances of the conductive network. Therefore, this approach could lead to higher loading of sulfur electrode and significantly improved cycling stability

2.2 Battery Performance

To *in situ* verify polysulfide immobilization capability during Li-S battery operation, the polymers were assembled into coin cells as S cathode binders. In designing the polymeric electrode, both nano- and micron-size sulfur particles are applied as active material along with

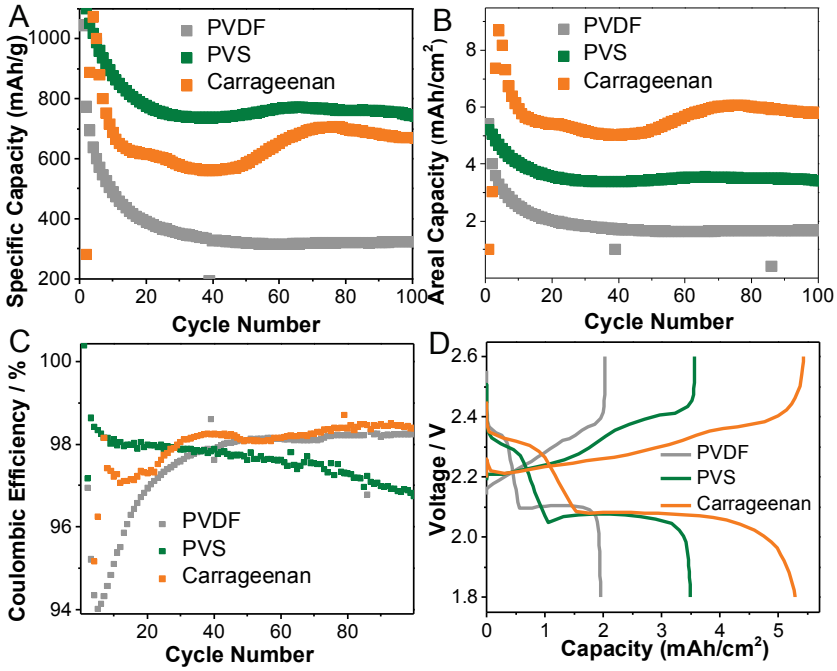

Fig. 3. Li-S battery testing results of micron-S electrodes made with different polymers. (A,B) Cycling performance of high-loading sulfur electrodes based on PVDF, PVS, carrageenan at 0.05C. The sulfur loadings of the electrode are around 5-10 mg, and the thickness around 200 μm. (C) Coulombic efficiencies varies. PVDF shows worst efficiency at the early cycles due to excessive polysulfide shuttles. PVS has very good coulombic efficiency due to the initial fast reaction of PVS with polysulfide. Carrageenan gives consistently good cycling efficiency. (D) discharge/charge voltage profiles between 1.8-2.6 V at 10th cycles. The two-plateau discharge behavior shows the formation of long chain polysulfide in the charge state.

the polymer binder and conductive carbon additives. The electron conductive matrix is formed by the percolated carbon conductive additive particles held together by polymer binders. The polymer thickness is around 3 nm (calculated) on the surface of the conductive particles, which is well within the electron-tunneling limit [53].

The galvanostatic cycling profiles are shown in Fig. 3. In contrast to PVDF, the electrodes achieved remarkable performance with PVS and carrageenan polymer binders. The relative ratio between sulfur and liquid affects the cycling stability of Li-S batteries.[54] Increase the amount of electrolyte tends to improve sulfur electrode performance by improving the Li-ion and the polysulfides mobility. However these increased motilities negatively affect the lithium metal electrode. The optimum ratio between solid sulfur and

liquid electrolyte was identified to be 50 g L^{-1} (20 μL/mg-s).[55] This optimum highly depends on sulfur loading, and electrode materials choice. In our work, high loading of sulfur is used in the electrode, 16 μL/mg-s generate best results, and has been consistently used in this study. The carrageenan binder electrode achieved a first discharge capacity of 8.8 mAh/cm^2. The capacity was maintained at approximately 6 mAh/cm^2 for more than 140 cycles, corresponding to a specific capacity of approximately 700 mAh/g (Fig. 3A, B; Fig. S4). Electrode thickness was 200 μm. The capacity revival after around 40 cycles is due to the electrolyte uptake. The penetration of electrolyte in the thick electrode is a slow process. After full wetting around 40 cycles, the ionic conductivity reaches a maximum, in turn improves capacity.[55] In comparison, cells using PVDF binder suffered from rapid capacity decay, showing capacity retention of 31% after 100 cycles. The PVS also gave initial good performance. The specific capacity using the PVS binder was 100 mAh/g higher than carrageenan, initially. However, due to the poor adhesion strength of PVS with the carbon conductive additive, the capacity decayed faster than the test using carrageenan binder, although performance was still better than tests using PVDF.[16] The average coulombic efficiency of the carrageenan electrodes is more than 98% over 100 cycles, the best among the three binders tested (Fig. 3C).

The number of nucleophilic substitution reaction sites in each carrageenan repeating unit is 3 according to Fig. 1A. To trap all the sulfur in the electrode in the form of C-S_8Li, the weight ratio of sulfur to binder should be around 5/4. Since the polymer does not contribute to capacity, the ratio of sulfur to binder is fixed at 5/1 to achieve higher capacity in the electrode. The nucleophilic substitution reaction is irreversible to form a permanent chemical bond between the carbon and sulfur (C-S). There is an irreversible sulfur species loss due to the formation of C-S bond, depending on the ratio of sulfur to binder materials. The irreversible capacity loss of active sulfur is calculated to be only 1.5 wt% at the sulfur to carrageenan binder ratio of 5/1, assuming all the sulfate groups are substituted by the LiS_8^-, and the attached segment is C-S_8Li. The segment can still be reduced to Li_2S, except the S directly connected to the C. It will reduce to C-SLi form. Only 3 wt% of sulfur is attached to the binder in the C-S form. However, this attached C-S species is uniformly distributed in the binder. The consumption of sulfur species by forming the C-S bond is small. During

discharge, more low-order of polysulfide will be formed and may not bind with the polymer, therefore their diffusion into electrolyte is possible. However the C-SLi sites provide anchor points on the cathode for the high order of polysulfide to attach when the polysulfide is at the maximum possibility to dissolve. These C-SLi sites can also provide a precipitation points for the discharged Li_2S species.[56]

As shown in Figure 3D, two well-defined discharge plateaus are observed, which are assigned to the multistep reduction mechanism of elemental sulfur. The first plateau, centered at around 2.3 V is generally attributed to the reduction of neutral sulfur species and formation of S_8^{2-}. The later plateau is ascribed to the further reduction of higher polysulfides (Li_2S_n, $4 \leq n \leq 8$) to the lower polysulfides (Li_2S_n, $n \leq 3$) [32]. This double plateau behavior of both PVS- and carrageenan-based electrodes shows the formation of S_8^{2-}, and other longer chain ($n > 8$) sulfur species in every cycle even though the sulfur is bonded with polymer backbones. The sulfur electrode behavior is distinctively different from pre-synthesized carbon sulfur composite materials [12, 21, 57]. Fig. S4 displays the rate performance for the carrageenan-based electrode. Even at a higher current density of 0.55 A/g (or C/3), the electrode was able to maintain a capacity of 3 mAh/cm^2 for more than 100 cycles.

According to the study by Yuriy et al.,[6] the delithiation shuttle factor can be described in the following equation:

$$\frac{k_S q_H [S_{total}]}{I_d} = f_d$$

k_s is the shuttle constant, q_H is the high plateau sulfur specific capacity, $[S_{total}]$ is the total sulfur concentration, I_d is the delithiation current, f_d is the delithiation-shuttle factor. At

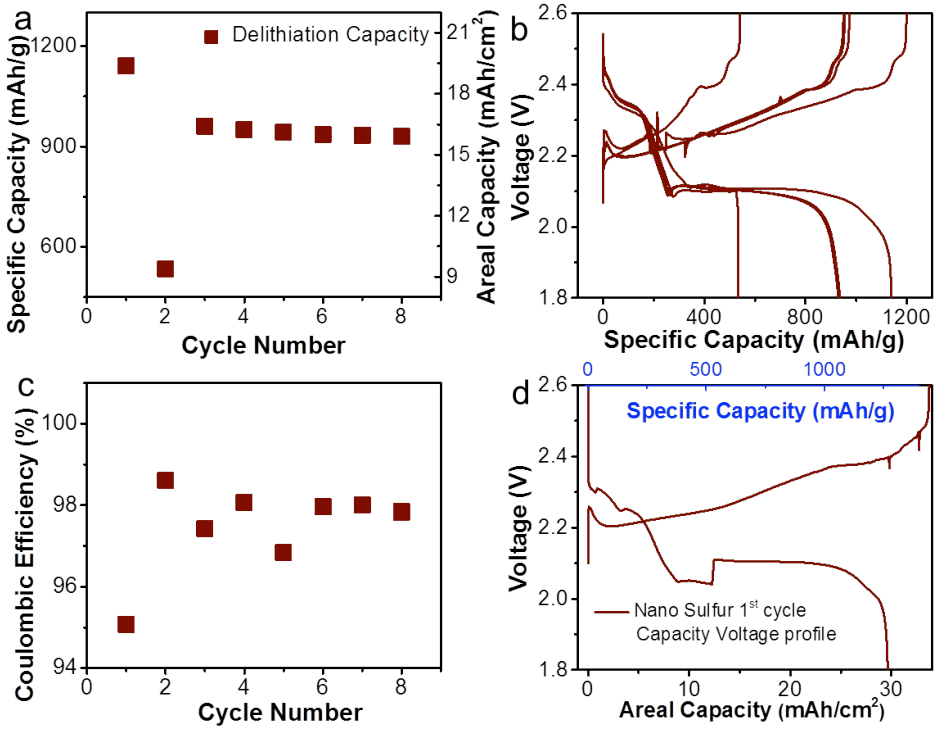

Fig. 4. Electrochemical performance of carrageenan based micro- and nano-sulfur electrodes. A,B) Reversible capacity of 17.0 mg/cm^2 micon-sulfur mass loading electrodes based on carrageenan at 0.01C. C) Coulombic efficiency of the carrageenan based micro-sulfur electrode. D) The initial capacity voltage profile of carrageenan based nano-sulfur electrode with the sulfur mass loading of 24.6 mg/cm^2.

$k_s q_H [S_{total}]/I_d$<1, when the shuttle constant is low or the charge current is high enough, the cell could be fully delithiated, showing a sharp voltage increase. Rather, at $k_s q_H [S_{total}]/I_d$>1, the cell never reaches complete delithiation and shows a voltage leveling. Hence, to further demonstrate the low shuttle constant of carrageenan based sulfur electrodes, the mass loading of sulfur was further increased to 17.0 mg/cm^2 and cycled at an even low current density of 0.01C. As plotted in Fig. 4A and B, the initial delithiation capacity is 1199.1 mAh/g, equals to 20.4 mAh/cm^2. The capacity was stabilized at 940 mAh/g and 16 mAh/cm^2 in the following cycles. The comparison between various polymers binder indicates that the shuttle constant for carrageenan based cell is curtailed and controlled even at such a high sulfur concentration and low charge current. Besides, sulfur particle size effect is also investigated as shown in Fig 4D. A further increase of the areal capacity of 33.7 mAh/cm^2 is achieved based on 24.6

mg/cm^2 nano-sulfur mass loading electrode. The calculated sulfur utilization is 81.8% based on the specific capacity of 1368.5 mAh/cm^2. The smaller particle size facilitate more effective contact point between the polymers and sulfur elements.

To summarize the benefits of the nucleophilic reaction during cycling, the whole process is described as below: large sulfur particles gradually form polysulfide via both electrochemical as well as chemical process. The long-chain polysulfide will instantaneously react with the polymer binders in the electrode via a nucleophilic substitution reaction mechanism to form an immobilized/grafted/crosslink polysulfide and polymer network. Therefore, this nucleophilic substitution reaction process is electrochemically activated. This grafted polysulfide is part of the polymer binders, so much closer to the conductive network. The grafted polysulfide can continuously react in the charging process to form non-soluble short-chain polysulfide, which distributes within the conductive network. Upon charging (delithiation), the long-chain polysulfide re-forms. However, now the C-S bond is stable [58-59] in the polysulfide reduction and oxidation process, providing anchor points for sulfide grafting and immobilization. This novel chemistry process addresses the challenge of polysulfide dissolution and the shuttle effect, and eventually solves the polysulfide dissolution issue. Other types of functional polymers with the potential to have nucleophilic reaction with polysulfide can be further identified and applied based on the same principal.

In addition to chemical binding and adhesion strength, polymer distribution uniformity is also very important. Both optical image and atomic force microscopy (AFM) are used to study the surface uniformity of the drop-cast polymer films (Fig. S6, S7). The surface of PVS is much rougher than that of carrageenan in the optical image. In the AFM surface images, the carrageenan film shows much smaller surface aggregation than that of the PVS (Fig. S6). This film roughness may translate to uneven distribution of binder in the composite electrode, hindering electron mobility in the PVS composite [60]. The microscopic images by SEM of composite electrodes made with carrageenan are shown in Fig. S7 and S8. The micron-size

sulfur particles are transformed and redistributed evenly in the composite electrode after the first charging process.

To evaluate the electrode morphology evolution during the cycling process, scanning electron microscopies (SEM) are taken of the non-cycled electrode *vs*. the cycled electrode at different state of charges (Fig. S8 and S9). When the cells are disassembled at a fully discharged state, no delamination of the electrode and none of the polysulfide deep yellow color in the electrolyte were found. The micron-size large sulfur particles disappear. A homogeneous Li_2S accumulation in the electrode pores is visible, indicating good conductivity of the electrode and uniform Li_2S deposition due to grafting of polysulfide on the polymer binder. Moreover, in charge state, the electrode returns to its highly porous state and the micron-size sulfur particles do not reappear. The sulfur deposition is uniformly distributed onto the grafted polymers. These results show an innovative polymer chemistry approach successfully applied to solve the lithium polysulfide shuttle effect using a nucleophilic substitution reaction of C-S bond formation to graft long-chain polysulfide to the polymer binder. Polysulfide grafting prevents the shuttle effect and stabilizes capacity.

2.3 Operando Li-S system observation.

In the material level, nucleophilic substitution reaction is very effective in immobilizing polysulfide in the polymer network. In the system level, Li-S cell performance also confirms the effectiveness of this reactive polymer approach. In addition, the *operando* synchrotron-based XAS experiments are designed to monitor the polysulfide formation and capturing using both carrageenan polymers and a non-reactive PVDF polymer. This *operando* test allows further understanding of the polymer binder reactivity to polysulfide activities in a real operational cell.[61]

The *operando* cell setup and measurement are illustrated in Fig. 5A. A series of coin cells with a polyimide film-sealed window on the sulfur electrode side are designed for X-ray penetration. The *operando* XAS spectra are collected using total fluorescence yield (TFY)

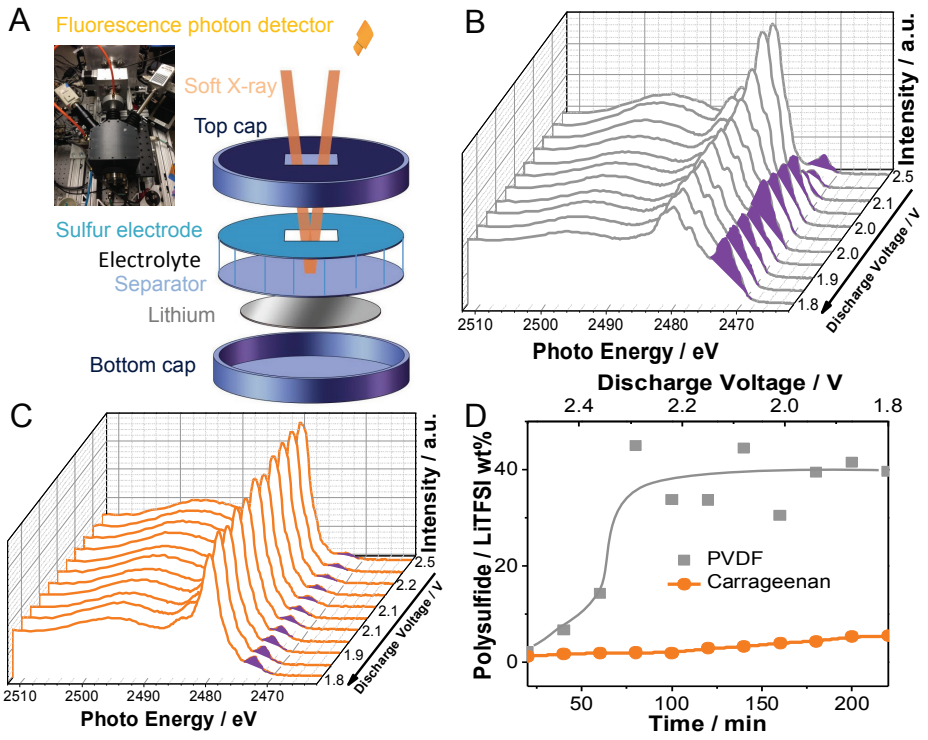

Fig. 5. *Operando* XAS measurements of Li-S cell. (A) Schematic of the *in situ* XAS measurement set-up. The inlet photo is the actual customer build instrumentation for this experiment. (B,C) The S K-edge XAS spectra evolution of the electrolyte with voltage scan. The purple highlighted peaks are polysulfide adsorption peaks, which evolve during first discharge. PVDF binder based Li-S cell shows the dramatic increase of polysulfide concentration in the electrolyte during the first lithiation process. The carrageenan binder based Li-S cell shows much slow concentration built up of polysulfide. D) The relative polysulfide concentration changes with discharge shows the superiority of carrageenan binder in immobilizing polysulfide.

mode and calibrated using elemental sulfur spectra assuming the white line to be at 2472.2 eV [50]. The cells are continually galvanostatically discharged from the initial 2.6V to 1.8V at a C-rate equivalent to C/5, while monitoring the fluorescence spectra. The peak area at 2480.0 eV [62] is proportional to the concentration of the LiTFSI in the electrolyte. Since the LiTFSI concentration does not change much, it absorbance is defined as a unit to calculate the relative concentration of polysulfide. Therefore, the contribution of dissolved Li_2S_x, elemental sulfur, and other polysulfide species are recorded in TFY and compared with intensity of LiTFSI. When an inert PVDF polymer binder is used, the polysulfide concentration increases rapidly starting around 2 V, when the discharge starts. The concentration reaches a high plateau quickly and stays at high concentration throughout the end of the discharge process (to 1.8 V). This polysulfide dissolution is consistent with previous literature.

However, when a reactive carrageenan polymer binder is used, the reaction between the polysulfide and carrageenan polymer effectively immobilize the polysulfide within the cathode electrode; the concentration of polysulfide is very low throughout the discharge process to the sulfur electrode (Fig. 5C). A very slow concentration build up of polysulfide in the electrolyte is observed in the case of the carrageenan-based sulfur electrode, although both carrageenan- and PVDF-based electrodes have the same composition. As shown in Fig. 5D, the concentration of sulfur species in the electrolyte for carrageenan-based sulfur electrode stays very low, compared to that of the PVDF-based electrode during the voltage scan at extended time period.

The *operando* experiments further confirm what is observed in the polysulfide reaction with polymer: fast polysulfide nucleophilic substitution reactions with the leaving groups on the polymers binder. The effective immobilization of polysulfide in the electrode resulting in crosslink structure provides superb prevention of polysulfide dissolution. This chemical reaction initiates by the first electrochemical discharge without generating adverse species to the Li-S chemistry.

3. Conclusions

A radically different approach is developed and demonstrated in this research: instead of the popular sulfur confinement and physical absorption approach, this work relies on a multifunctional reactive polymer as a grafting agent and binder for its success. The project team started with a chemically designed and synthesized PVS polymer, and then moved to a nature-inspired aqueous-based carrageenan polymer with designed functional groups and improved adhesion. The polymer forms a conductive network with carbon black, but also reacts with polysulfide to form sulfur-grafted polymer when first used in a Li-S battery. These carrageenan polymer binders can continuously react with any polysulfide when it breaks free into the electrode during the operation of the battery. The polysulfide concentration remains very low in the electrolyte during the operation. The process immobilizes the polysulfide to prevent dissolution, but also crosslinks the polymer binder to potentially provide additional

mechanical stability of the conductive network. It also brings the sulfide closer to the charge transfer sites.

This approach is simple, effective and initiated at the first discharge of the battery. No additional processing is required for the sulfur, and the binder is a water-soluble natural product that is already used as a food additive. In the current stage, Li-S batteries still require lithium metal electrode stabilization for the long and safe use of the battery. However, this approach opens up new horizons for sulfur electrodes. Currently the lithium-ion slurry process is used to make the sulfur electrode, but this research may lead to using classic low-cost polymer extrusion process to make the sulfur electrode with high polymer content and using a stamping process to make ion transport channels in sulfur electrodes. The polymer binder is no longer an inactive species as in lithium ion cells, but it is active in retaining sulfur, hence retaining capacity. Introducing high content of polymer binders will further stabilize capacity by depressing sulfur dissolution, but with a resulting lower energy-density. However, the lower cost materials and processes will more than compensate for the sacrifices in energy-density. Therefore, this type of sulfur battery may be able to find wide applications in stationary storage applications that are cost sensitive but can tolerate reduced energy-density for battery life performance.

ACKNOWLEDGMENT

This work was supported by the Assistant Secretary for Energy Efficiency and Renewal Energy under the Battery Materials Research (BMR) program. X-ray Adsorption Spectroscopy and analyses were performed at the Advanced Light Source (ALS); UV-Vis and XPS analyses at the Molecular Foundry - all are located at Lawrence Berkeley National Laboratory, and supported by the Office of Science, Office of Basic Energy Sciences, of the U.S. Department of Energy under contract no. DE-AC02-05CH11231, National Key Research and Development Program of China (2016YFA0202603), National Natural Science Fund for Distinguished Young Scholars (51425204).

ASSOCIATED CONTENT

Supporting Information

Materials and Methods, Figures S1-S10.

References:

1. Dunn, B.; Kamath, H.; Tarascon, J. M. *Science* 334 (2011) 928-935.
2. Song, M. K.; Cairns, E. J.; Zhang, Y. G. *Nanos.* 5 (2013) 2186-2204.
3. Manthiram, A.; Fu, Y. Z.; Su, Y. S. *Acc. Chem. Res.* 46 (2013) 1125-1134.
4. Ji, X. L.; Evers, S.; Black, R.; Nazar, L. F. *Nature Communications* 2 (2011) DOI: 10.1038/ncomms1293.
5. Manthiram, A.; Fu, Y. Z.; Chung, S. H.; Zu, C. X.; Su, Y. S. *Chem. Rev.* 114 (2014) 11751-11787.
6. Mikhaylik, Y. V.; Akridge, J. R. *J. Electrochem. Soc.* 151 (2004) A1969-A1976.
7. Yin, Y. X.; Xin, S.; Guo, Y. G.; Wan, L. J. *Angew. Chem. Int. Edit.* 52 (2013) 13186-13200.
8. Wu, F.; Qian, J.; Chen, R. J.; Zhao, T.; Xu, R.; Ye, Y. S.; Li, W. H.; Li, L.; Lu, J.; Amine, K. *Nano Energy* 12 (2015) 742-749.
9. Song, J.; Gordin, M. L.; Xu, T.; Chen, S.; Yu, Z.; Sohn, H.; Lu, J.; Ren, Y.; Duan, Y.; Wang, D. *Angew. Chem. Int. Edit.* 54 (2015) 4325-9.
10. Li, Z.; Jiang, Y.; Yuan, L. X.; Yi, Z. Q.; Wu, C.; Liu, Y.; Strasser, P.; Huang, Y. H. *ACS Nano* 8 (2014) 9295-9303.
11. Peng, H. J.; Huang, J. Q.; Zhao, M. Q.; Zhang, Q.; Cheng, X. B.; Liu, X. Y.; Qian, W. Z.; Wei, F. *Adv. Funct. Mater.* 24 (2014) 2772-2781.
12. Schuster, J.; He, G.; Mandlmeier, B.; Yim, T.; Lee, K. T.; Bein, T.; Nazar, L. F. *Angew. Chem. Int. Edit.* 51 (2012) 3591-3595.
13. Zhu, L.; Peng, H. J.; Liang, J. Y.; Huang, J. Q.; Chen, C. M.; Guo, X. F.; Zhu, W. C.; Li, P.; Zhang, Q. *Nano Energy* 11 (2015) 746-755.
14. Wang, J. G.; Xie, K. Y.; Wei, B. Q. *Nano Energy* 15 (2015) 413-444.
15. Chen, J. Z.; Wu, D. X.; Walter, E.; Engelhard, M.; Bhattacharya, P.; Pan, H. L.; Shao, Y. Y.; Gao, F.; Xiao, J.; Liu, J. *Nano Energy* 13 (2015) 267-274.
16. Wang, Z. Y.; Dong, Y. F.; Li, H. J.; Zhao, Z. B.; Wu, H. B.; Hao, C.; Liu, S. H.; Qiu, J. S.; Lou, X. W. *Nature Communications* 5 (2014) DOI: 10.1038/ncomms6002.
17. Cheng, X. B.; Huang, J. Q.; Zhang, Q.; Peng, H. J.; Zhao, M. Q.; Wei, F. *Nano Energy* 4 (2014) 65-72.
18. Huang, J. Q.; Liu, X. F.; Zhang, Q.; Chen, C. M.; Zhao, M. Q.; Zhang, S. M.; Zhu, W. C.; Qian, W. Z.; Wei, F. *Nano Energy* 2 (2013) 314-321.
19. Candelaria, S. L.; Shao, Y. Y.; Zhou, W.; Li, X. L.; Xiao, J.; Zhang, J. G.; Wang, Y.; Liu, J.; Li, J. H.; Cao, G. Z. *Nano Energy* 1 (2012) 195-220.
20. Ji, X. L.; Lee, K. T.; Nazar, L. F. *Nat. Mater.* 8 (2009) 500-506.
21. Wang, J. L.; Yang, J.; Xie, J. Y.; Xu, N. X. *Adv. Mater.* 14 (2002) 963-965.
22. Wang, H. L.; Yang, Y.; Liang, Y. Y.; Robinson, J. T.; Li, Y. G.; Jackson, A.; Cui, Y.; Dai, H. J. *Nano Lett.* 11 (2011) 2644-2647.
23. Wang, J.; Yao, Z.; Monroe, C. W.; Yang, J.; Nuli, Y. *Adv. Funct. Mater.* 23 (2013) 1194-1201.
24. Liu, X.; Huang, J. Q.; Zhang, Q.; Mai, L. *Adv Mater* (2017) DOI: 10.1002/adma.201601759.
25. Trofimov, B. A.; Morozova, L. V.; Markova, M. V.; Mikhaleva, A. I.; Myachina, G. F.; Tatarinova, I. V.; Skotheim, T. A. *J. Appl. Polym. Sci.* 101 (2006) 4051-4055.
26. Huang, Y.; Sun, J.; Wang, W.; Wang, Y.; Yu, Z.; Zhang, H.; Wang, A.; Yuan, K. *J. Electrochem. Soc.* 155 (2008) A764.
27. Wang, Q.; Wang, W.; Huang, Y.; Wang, F.; Zhang, H.; Yu, Z.; Wang, A.; Yuan, K. *J. Electrochem. Soc.* 158 (2011) A775.
28. Zhang, W.; Huang, Y.; Wang, W.; Huang, C.; Wang, Y.; Yu, Z.; Zhang, H. *J. Electrochem. Soc.* 157 (2010) A443.
29. Lacey, M. J.; Jeschull, F.; Edström, K.; Brandell, D. *J. Power Sources* 264 (2014) 8-14.

30. Zhang, Z.; Bao, W.; Lu, H.; Jia, M.; Xie, K.; Lai, Y.; Li, J. *ECS Electrochem. Lett.* 1 (2012) A34-A37.
31. He, M.; Yuan, L.-X.; Zhang, W.-X.; Hu, X.-L.; Huang, Y.-H. *J. Phys. Chem. C* 115 (2011) 15703-15709.
32. Seh, Z. W.; Zhang, Q.; Li, W.; Zheng, G.; Yao, H.; Cui, Y. *Chem. Sci.* 4 (2013) 3673-3677.
33. Li, G.; Ling, M.; Ye, Y.; Li, Z.; Guo, J.; Yao, Y.; Zhu, J.; Lin, Z.; Zhang, S. *Adv. Energy Mater.* 5 (2015) 1500878.
34. Bhattacharya, P.; Nandasiri, M. I.; Lv, D. P.; Schwarz, A. M.; Darsell, J. T.; Henderson, W. A.; Tomalia, D. A.; Liu, J.; Zhang, J. G.; Xiao, J. *Nano Energy* 19 (2016) 176-186.
35. Ai, G.; Dai, Y.; Ye, Y.; Mao, W.; Wang, Z.; Zhao, H.; Chen, Y.; Zhu, J.; Fu, Y.; Battaglia, V.; Guo, J.; Srinivasan, V.; Liu, G. *Nano Energy* 16 (2015) 28-37.
36. Cheng, H.; Wang, S. P. *Journal of Materials Chemistry A* 2 (2014) 13783-13794.
37. Takano, R.; Shiomoto, K.; Kamei, K.; Hara, S.; Hirase, S. *Bot. Mar.* 46 (2003) 142-150.
38. Necas, J.; Bartosikova, L. *Vet. Med.* 58 (2013) 187-205.
39. Chou, S. L.; Pan, Y. D.; Wang, J. Z.; Liu, H. K.; Dou, S. X. *Phys. Chem. Chem. Phys.* 16 (2014) 20347-20359.
40. Genesty, M.; Degrand, C. *New J. Chem.* 22 (1998) 349-354.
41. Hoye, T. R.; Crawford, K. B. *J. Org. Chem.* 59 (1994) 520-522.
42. Livneh, M.; Sutter, J. K.; Sukenik, C. N. *J. Org. Chem.* 52 (1987) 5039-5041.
43. Kawase, A.; Shirai, S.; Yamoto, Y.; Arakawa, R.; Takata, T. *Phys. Chem. Chem. Phys.* 16 (2014) 9344-9350.
44. Bartsch, R. A.; Bunnett, J. F. *J. Am. Chem. Soc.* 90 (1968) 408.
45. Lee, J. G.; Bartsch, R. A. *J. Am. Chem. Soc.* 101 (1979) 228-229.
46. Vasaros, L.; Norseyev, Y. V.; Nhan, D. D.; Khalkin, V. A. *Radiochem. Radioa. Lett.* 47 (1981) 403-407.
47. Feng, X. F.; Song, M. K.; Stolte, W. C.; Gardenghi, D.; Zhang, D.; Sun, X. H.; Zhu, J. F.; Cairns, E. J.; Guo, J. H. *Phys. Chem. Chem. Phys.* 16 (2014) 16931-16940.
48. Lorenz, O.; Parks, C. R. *J. Polym. Sci.* 50 (1961) 299-312.
49. Dey, A.; Chow, M.; Taniguchi, K.; Lugo-Mas, P.; Davin, S.; Maeda, M.; Kovacs, J. A.; Odaka, M.; Hodgson, K. O.; Hedman, B.; Solomon, E. I. *J. Am. Chem. Soc.* 128 (2006) 533-541.
50. Griebel, J. J.; Li, G. X.; Glass, R. S.; Char, K.; Pyun, J. *J. Polym. Sci. A* 53 (2015) 173-177.
51. Lin, C. N.; Chen, W. C.; Song, Y. F.; Wang, C. C.; Tsai, L. D.; Wu, N. L. *J. Power Sources* 263 (2014) 98-103.
52. Martin-Diaconescu, V.; Kennepohl, P. *J. Am. Chem. Soc.* 129 (2007) 3034-3035.
53. Sheehy, B.; Lafon, R.; Widmer, M.; Walker, B.; DiMauro, L. F.; Agostini, P. A.; Kulander, K. C. *Phys. Rev. A* 58 (1998) 3942-3952.
54. Rosenman, A.; Markevich, E.; Salitra, G.; Aurbach, D.; Garsuch, A.; Chesneau, F. F. *Adv. Energy Mater.* 5 (2015). DOI: 10.1002/aenm.201500212.
55. Zheng, J.; Lv, D.; Gu, M.; Wang, C.; Zhang, J. G.; Liu, J.; Xiao, J. *J. Electrochem. Soc.* 160 (2013) A2288-A2292.
56. Chung, W. J.; Griebel, J. J.; Kim, E. T.; Yoon, H.; Simmonds, A. G.; Ji, H. J.; Dirlam, P. T.; Glass, R. S.; Wie, J. J.; Nguyen, N. A.; Guralnick, B. W.; Park, J.; Somogyi, A.; Theato, P.; Mackay, M. E.; Sung, Y. E.; Char, K.; Pyun, J. *Nat. Chem.* 5 (2013) 518-524.
57. Ye, Y.; Kawase, A.; Song, M.-K.; Feng, B.; Liu, Y.-S.; Marcus, M. A.; Feng, J.; Fang, H.; Cairns, E. J.; Zhu, J.; Guo, J. *J. Phys. Chem.C* 120 (2016) 10111-10117.
58. Wagner, F. C.; Reid, E. E. *J. Am. Chem. Soc.* 53 (1931) 3407-3413.

59. Kondo, T.; Mitsudo, T. *Chem. Rev.* 100 (2000) 3205-3220.
60. Park, S.-J.; Zhao, H.; Ai, G.; Wang, C.; Song, X.; Yuca, N.; Battaglia, V. S.; Yang, W.; Liu, G. *J. Am. Chem. Soc.* 137 (2015) 2565-2571.
61. Nelson, J.; Misra, S.; Yang, Y.; Jackson, A.; Liu, Y. J.; Wang, H. L.; Dai, H. J.; Andrews, J. C.; Cui, Y.; Toney, M. F. *J. Am. Chem. Soc.* 134 (2012) 6337-6343.
62. Cuisinier, M.; Cabelguen, P. E.; Evers, S.; He, G.; Kolbeck, M.; Garsuch, A.; Bolin, T.; Balasubramanian, M.; Nazar, L. F. *J. Phys.Chem. Lett.* 4 (2013) 3227-3232.